

## EXPERIMENTAL STUDY FOR ESTIMATING TSUNAMI FORCES ACTING ON BRIDGE GIRDERS

Kenji Kosa<sup>1</sup>, Shinichi Nii<sup>2</sup>, Kenta Miyahara<sup>3</sup>, and Manabu Shoji<sup>4</sup>

### **Abstract**

An experiment was conducted to evaluate wave forces acting on bridges due to tsunami. Two types of waveforms, broken waves and unbroken waves, were used in the experiment. In the case of broken waves, the horizontal force was stronger than the uplift force. In the case of unbroken waves, the horizontal force was weaker than the uplift force. It was also found that the maximum horizontal wave force was 2.6 times as large as the hydrostatic pressure, and the maximum uplift force was 0.5 times as large as the hydrostatic pressure.

### **Introduction**

When tsunamis struck the northwestern region of Sumatra Island in Indonesia on Dec. 26, 2004, not only ordinary houses but also bridges were washed away. Such damage occurred to 81 bridges out of 168 that existed on the 250-km road section on the northwestern coast of Sumatra Island (Unjoh 2007).

Japan has a particular interest in tsunami damage to road structures because the Tokai (eastern sea) Earthquake and the Tounankai (southeastern sea) Earthquake are forecasted to hit the Pacific side of central Japan within the next 30~50 years. To address the issue, researchers and organizations are conducting research on tsunami damage to road structures.

Among the road structure damages on Sumatra Island, the authors focused on the wash-away of so many girders, and conducted an experiment to evaluate the tsunami forces acting on girders (Kosa 2009). The waves created in the experiment were sine wave-like waves, called one-crest solitary waves. This wave type was selected because it is the first wave of tsunami that has the possibility of wielding the strongest wave force. In the wave-making test, it was found that two types of wave forms can be created in the experimental tank: one is the wave that acts on the girder in an unbroken one crest form; the other is the wave that acts on the girder in a broken form with water splashes.

---

<sup>1</sup> Professor, Dept. of Civil Engineering, Kyushu Institute of Technology

<sup>2</sup> Engineer, Design Department, Wesco Co., Ltd.

<sup>3</sup> Graduate Student, Dept. of Civil Engineering, Kyushu Institute of Technology

<sup>4</sup> Assoc. Professor, Graduate School of Systems and Info. Eng., University of Tsukuba

In this report, we will present the features of wave actions that vary by waveforms firstly and then propose an equation for estimating the forces of acting waves based on the experimental results. The experimental parameters are the depth of static water, the distance between the static water level and the lower plane of the girder (hereinafter referred to as “girder height”), and the forms of waves (broken or not broken).

## **Experimental Program**

### **Tank, Girder Model, and Measuring Method**

A long tank, 41 m long, 80 cm wide, and 125 cm deep, was used for the experiment. One side of the tank is constructed of transparent glass to enable observation. Figure 1 shows the entire structure of the tank. The wave-making device on the left side is a slide type board controlled by PC. If the required wave height and initial water depth (the length between the tank bottom and the static water level) are inputted, PC will automatically perform calculation and determine the necessary force to push the wave-making board.

The girder model is a 1/50 scale model resembling an actual Indonesian bridge damaged by tsunami during the disaster. The girder model is 40 cm long, 19 cm wide, and 3.4 cm high (actual size of the damaged bridge: 19.1 m long, 10.2 m wide, and 1.7 m high). Two seabed slopes with a gradient of 1/20 were created in the tank to imitate an actual seabed.

Figure 2 shows the experimental setup around the model girder. The left figure shows a front view and the right figure a side view. One feature of this setup is that we placed a side wall on both sides of the girder model. They were placed to extract forces that act only on the girder by removing 3D type wave disturbances that would occur if abutments are located. The front side of the side walls was tapered to reduce wave disturbances that occur due to the collision of waves against the side walls. The measurement items were the wave height and acting forces on the girder. Six wave gauges were placed in the tank. Wave gauges H1 through H4 (Figs. 1 and 2) were used to measure the wave height that changes by the presence of seabed slopes. Wave gauge H5 (Fig. 2) was used to measure changes in wave height immediately after the collision of waves against the model. Wave gauge H6 was used to measure the height of waves that pass through between the side wall and transparent glass without being disturbed by the collision against the model. To measure these waves, wave gauge H6 was placed on the exterior side of the side wall but on the same centerline with the model, as seen in Fig. 2. The experimental results shown later were summarized using these waves. As the three-component balance, a 980N type was used. It can measure the horizontal wave force ( $F_x$ ) and the uplift force ( $F_z$ ). As shown in Fig. 3, a beam was fixed to the upper part of the tank and the balance was installed on it. Acting forces were measured via the jig. The balance and the jig were encased in the sheath to avoid wetting by waves. According to the rigidity verification test conducted separately, the natural period of the balance and the jig was about 30 Hz.

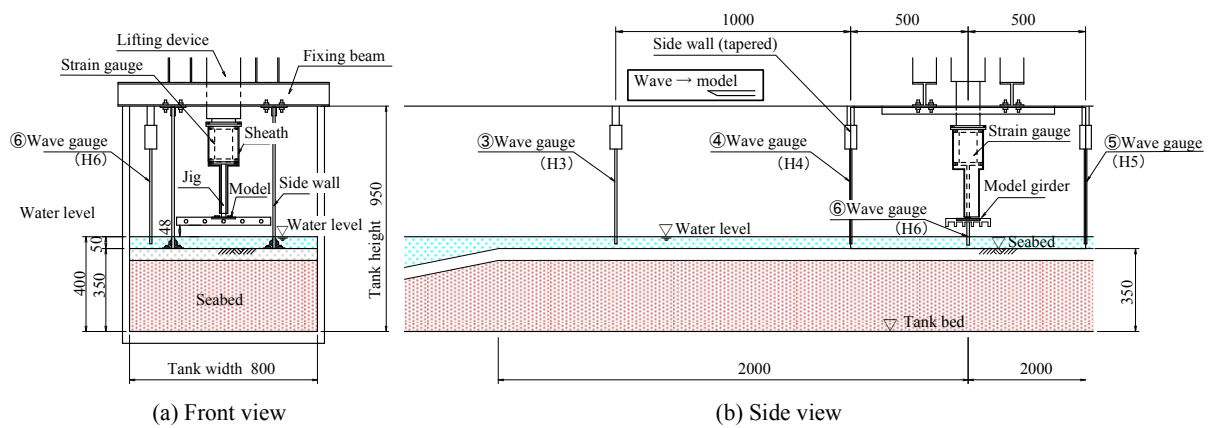
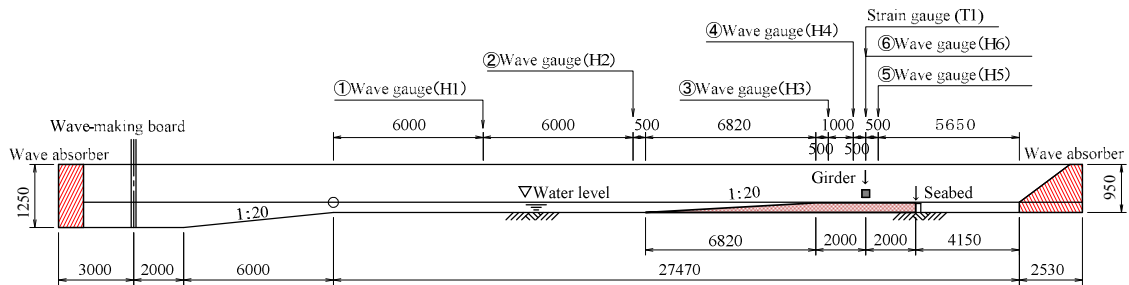
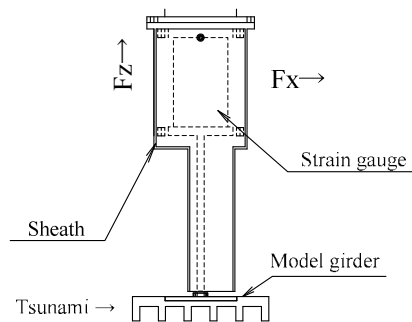


FIG. 2 EXPERIMENTAL SETUP



## Experimental Parameters

The experimental parameters were the forms of waves (broken or not broken), the depth of static water (length between the upper face of the seabed and the static water level) which was set based on the wave-making test on broken and unbroken waves, and the girder height which is the distance between the static water level and the lower plane of the girder.

Figure 4 shows the experimental conditions of the current experiment. The standard case (1/50 scale) was created by referring to the conditions of the actual damaged bridge in Indonesia. The static water depth of the standard case, which is 5 cm, is an equivalent depth determined from the actual water depth around the damaged bridge. Under those conditions, we attempted to produce 20 cm-high waves using a wave-making board to simulate an estimated 10 m-high waves that occurred during the disaster. In the experiment, the girder height was changed while the static water depth and the input wave height were kept constant.

The static water depth of the experimental cases was determined from the results of wave-making tests. In the current experiment, waves were created and controlled by PC. The input values were the wave height and the initial static water depth. In the wave-making test with a 5 cm water depth, all the waves got broken on the seabed. Therefore, we changed the static water depth to 15 cm and the input wave height to 7 cm. Then, we could obtain unbroken waves with one crest form. Because two types of waves were producible from the relationship between the input wave height and the static water depth, we prepared three experimental cases, as shown in Fig. 5: Case (1) - water depth 5 cm, input wave height 20 cm, broken waves; Case (2) - water depth 15 cm, input wave height 7 cm, unbroken waves; and Case (3) - water depth 15 cm, input wave height 20 cm, broken waves.

The input wave height of Case (1) was 20 cm, but the waves created were damped on the seabed, causing broken waves. When the waves arrived at the model girder, the wave height was reduced to about 10 cm. The input wave height of Case (2) was 7 cm and the waves passed through the model girder by retaining unbroken, convex-shaped one crest solitary waveform with a height of about 11 cm. The input wave height of Case (3) was 20 cm. The waves increased their height slightly on the seabed and became broken after reaching the top of the seabed. The waves passed through the model girder as if engulfing it with a wave height of 25 cm.

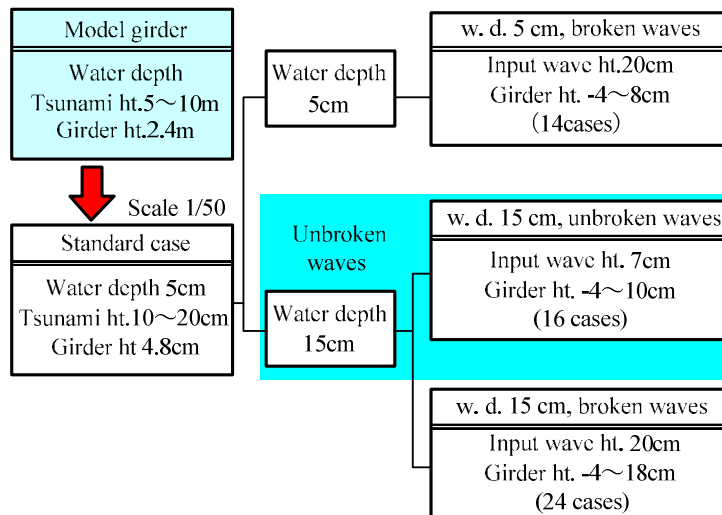


FIG. 4 EXPERIMENTAL FLOW

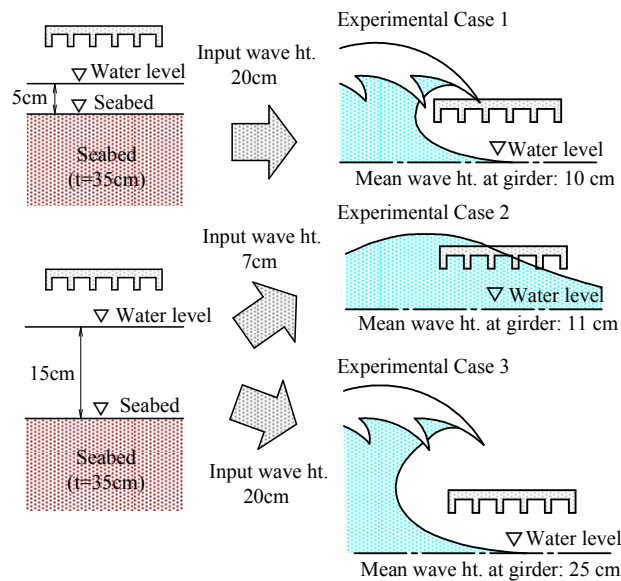


FIG. 5 WAVE TYPES OF EXPERIMENTAL CASES

### Evaluation Method of Experimental Results

Figure 6 shows a typical example of experimental results. The abscissa shows the time since the start of measurement and the ordinate shows the horizontal wave force that acted on the model girder. In this experiment, the sampling frequency was made to 1/1000 seconds. This frequency was selected to extract the momentary force when tsunami acts on

the model girder. According to the measurement data (1/1000 s) in Fig. 6, an amplitude with a natural period of about 0.041 seconds (frequency: 24 Hz) was observed after passing both the peak and 12 seconds from the start of measurement. It was confirmed that the natural period of the jig connected to a balance was about 30 Hz. So, the measured value might include the effect of resonance of the jig. Therefore, we removed that effect using a 1/10 sec. moving-mean method. The data after this treatment was roughly equal to the data which was obtained by removing (low-pass filter) the frequencies of over 5 Hz, which is 1/6 of the jig's resonance frequency of 30 Hz. The data treated by the 1/10 sec. moving-mean method is also shown in Fig. 6. It is seen that the maximum horizontal wave force is reduced to about 1/2. This treated data is used for the discussion of the experimental results in the following section.

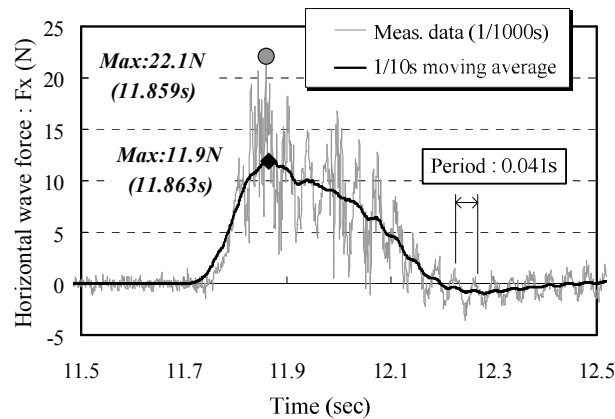


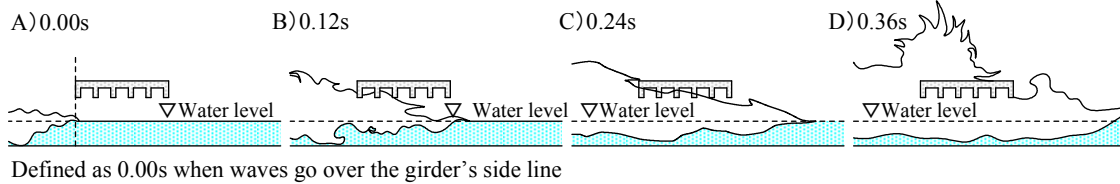
FIG. 6 HORIZONTAL WAVE FORCE AFTER PROCESSING BY MOVIN MEAN

## Experimental Results

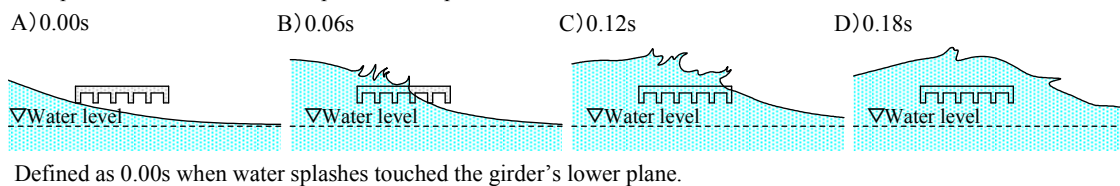
### Wave Actions in Each Experimental Case

Figure 7 shows the wave actions observed in the three experimental cases. The girder height was 4.8 cm in all cases. In Experimental Case (1) at the top of the figure, the waves broke before reaching the model girder and acted on the girder from the lower side in a state containing water bubbles. The wave height increased gradually and caused large water splashes when colliding against the girder. In Experimental Case (2) in the middle of the figure, waves did not break mostly even after colliding against the model girder and passed it by retaining one-crest waveform. In Experimental Case (3) at the bottom of the figure, the waves consisted of broken waves in the upper half and unbroken water mass in the lower half. The water splashes of broken waves acted on the upper plane of the model girder and then the unbroken water mass acted on the girder in a manner rolling it up in a clockwise direction from the lower left side.

① Experimental Case 1: water depth 5 cm, input wave ht. 20 cm, broken waves



② Experimental Case 2: water depth 15 cm, input wave ht. 7 cm, unbroken waves



③ Experimental Case 3: water depth 15 cm, input wave ht. 20 cm, broken waves

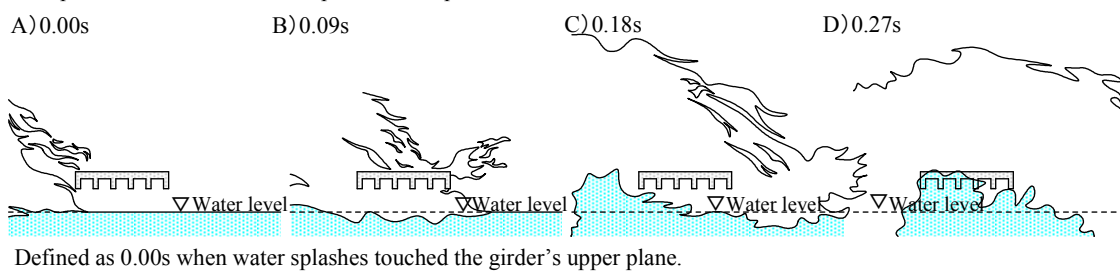


FIG. 7 WAVE ACTIONS ON THE GIRDER THAT VARY BY WAVEFORMS

### Acting Forces Varying by Broken or Unbroken Waves

Two measurement results are presented here. Figure 8 shows the measurement results of Experimental Case (1), namely, the horizontal wave force, uplift force, and wave height at the girder position. The wave height was measured in an uneven wave condition because the waves were broken when they acted on the girder. The horizontal wave force and the uplift force reached a peak around 11.4 seconds. After passing the peak, the uplift force turned to a negative value. This is because the water fell on the upper plane of the girder.

Figure 9 shows the results of Experimental Case (2). The wave height shows a smooth curve. The horizontal wave force and the uplift force reached a peak before the wave height became high. The feature was that the uplift force was roughly twice as large as the horizontal wave force.

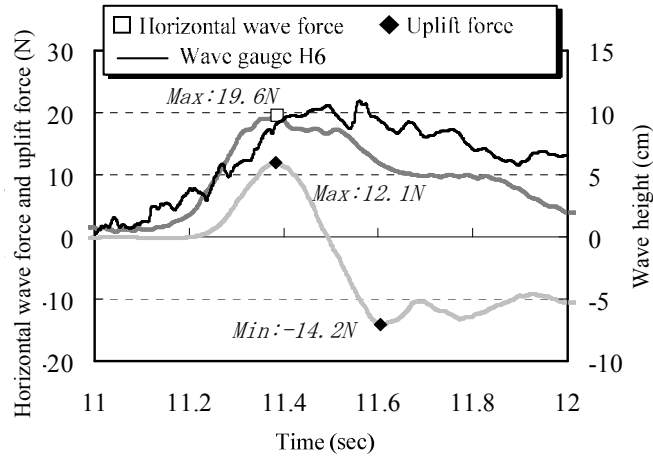


FIG. 8 ACTING FORCES AND WAVE HEIGHT (EXP. CASE 1)

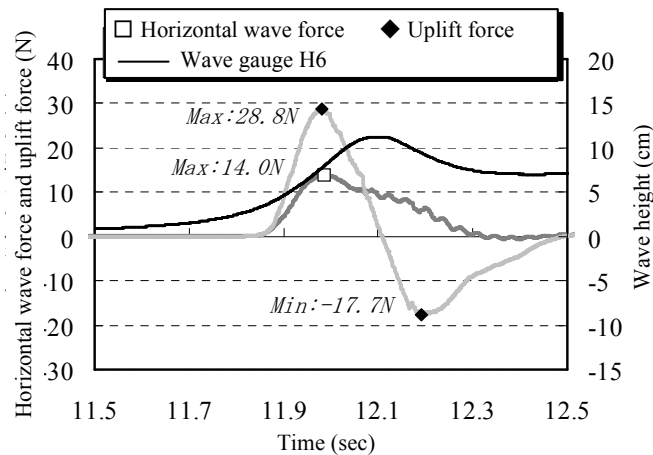


FIG. 9 ACTING FORCES AND WAVE HEIGHT (EXP. CASE 2)

### Features of Acting Forces that Vary by Waveforms

Figure 10 shows the results of Experimental Case (3). The abscissa shows the maximum value of acting forces and the ordinate shows the girder position. The waves in this Case consisted of broken and unbroken waves. The boundary between them was roughly at the middle point of the 25 cm mean wave height. According to the figure, the magnitude of horizontal and uplift forces reversed at the 12 cm position on the ordinate, which is roughly in agreement with the said boundary position.

Figure 11 shows the maximum value of horizontal wave force obtained from three experimental cases. The ordinate shows a dimensionless value obtained as a ratio of the girder center height to the wave height. And, the horizontal wave force was evaluated



using this ratio. It is seen that the largest horizontal wave force occurred in Experimental Case (3) that has the highest wave height. To simplify the observed features in Fig. 11, we produced Fig. 12 using the mean value of each experimental case. If Experimental Cases (1) and (2) are compared, it is known that the horizontal wave force became larger when the waves were broken even though the wave height was roughly the same. Figure 13 shows the results of uplift force obtained from a similar treatment with Fig. 12. According to the figure, the uplift force of Experimental Case (3) began to become small from around 0.4 on the ordinate and became smaller than that of Experimental Case (2).

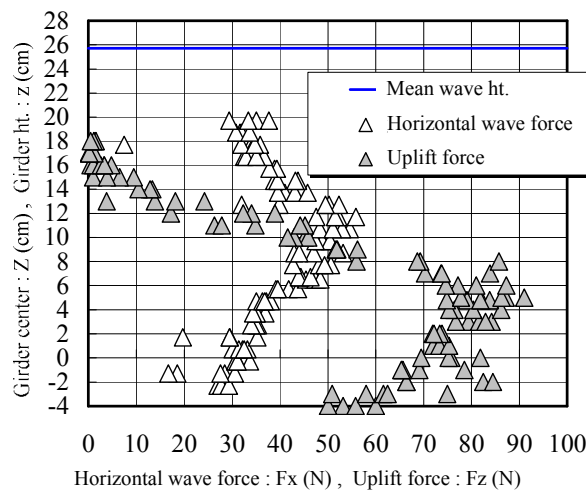


FIG. 10 GIRDER POSITION AND ACTING FORCES (EXP. CASE 3)

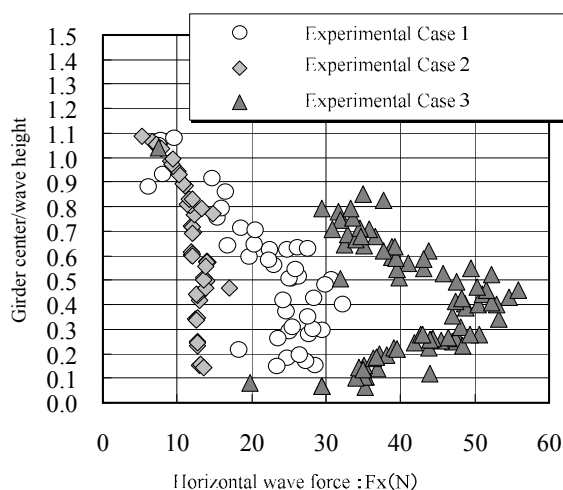


FIG. 11 GIRDER CENTER/WAVE HT. RATIO AND HORIZONTAL WAVE FORCE

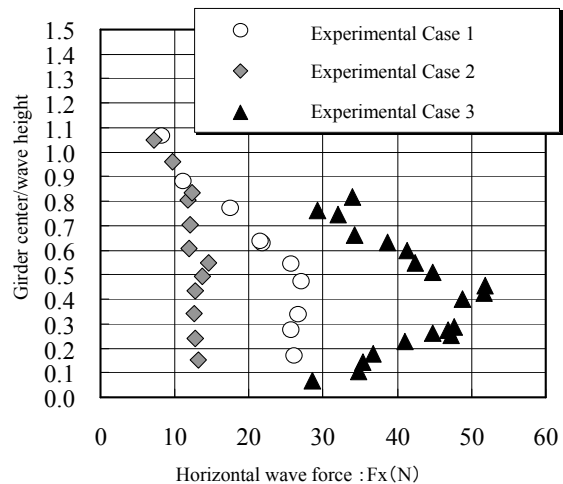


FIG. 12 GIRDER CENTER/WAVE HT. RATIO AND HORIZONTAL WAVE FORCE (MEAN)

Those tendencies are summarized in Fig. 14. When acting waves were not broken, the uplift force became larger than the horizontal force. When acting waves were broken, the uplift force became smaller than the horizontal force. However, the waves in Experimental Case (3) had both features. Namely, the features of acting forces that varied by waveforms, either broken or not, were observed, though the waveforms changed depending on the position of the girder.

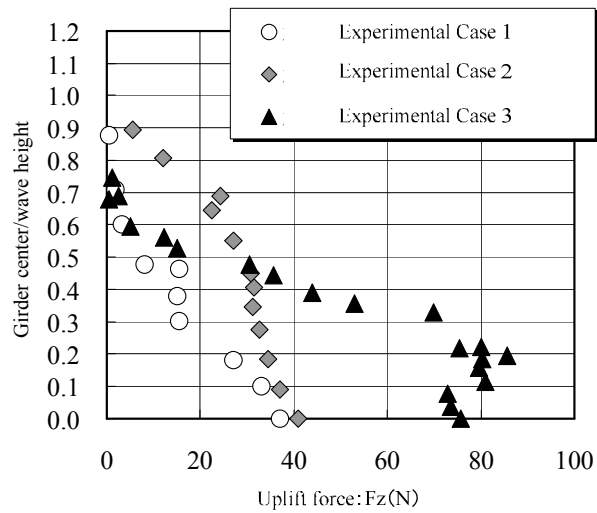


FIG. 13 GIRDER HT./WAVE HT. RATIO AND UPLIFT FORCE (MEAN)

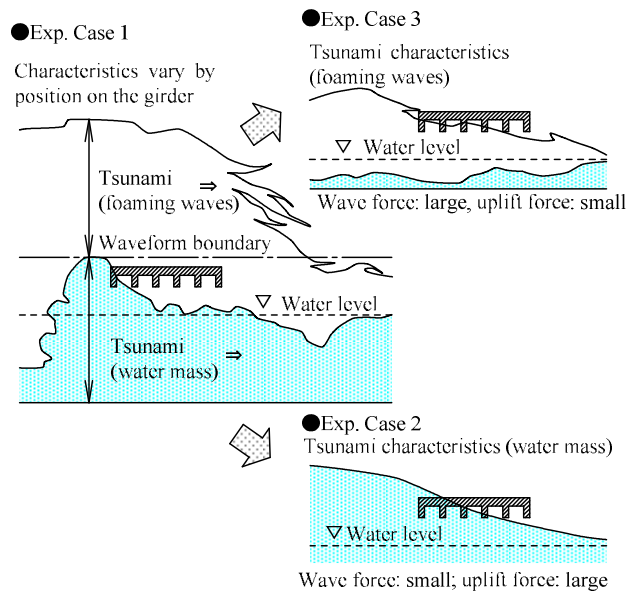


FIG. 14 CHARACTERISTICS OF ACTING FORCES THAT VARY BY WAVEFORM

## Evaluation of Experimental Results

Figures 15 and 16 are prepared from the horizontal forces and uplift forces in Figs. 12 and 13. The abscissa shows the dimensionless value obtained by dividing each acting force by the area of the possible receiving area (the side of the girder for the horizontal force, the lower plane of the girder for the uplift force) and the static water pressure against the tsunami height. The obtained values show the ratio to the static water pressure when the wave height was assumed as the water depth.

According to Fig. 15, the horizontal wave force against the static water pressure was the largest in Experimental Case (1). These results included the results of Experimental Case (3) that had a larger absolute horizontal wave force than Experimental Case (1). According to the results of uplift force in Fig. 16, the results of Experimental Case (2) included the results of the other two experimental cases. Based on this result, we obtained an approximate linear line and described it in each figure. For the calculation of those linear lines, the results of Experimental Case (1) (circle-marked values) were used for the horizontal force, and the results of Experimental Case (2) (diamond-marked values) were used for the uplift force. Here, we considered that “horizontal force/area of the girder’s side” and “uplift force/area of the girder’s lower plane” as the horizontal wave pressure ( $qx$ ) and vertical wave pressure ( $qz$ ) per  $m^2$ , respectively. Then, the abscissa of Fig. 15 becomes  $qx / \rho g a_H$  and the abscissa of Fig. 16 becomes  $qz / \rho g a_H$ . The approximation equation becomes as follows.

$$Z / a_H = - 0.54 (qx / \rho g a_H) + 1.41 \quad (1)$$

$$z / a_H = - 2.18 (qz / \rho g a_H) + 1.16 \quad (2)$$

where,       $Z$ : center of girder’s side plane       $a_H$ : wave height  
               $z$ : girder height (up to the lower plane of the girder)  
               $\rho$ : density of water       $g$ : gravitational acceleration  
               $qx$ : horizontal wave pressure       $qz$ : vertical wave pressure

The following equations are obtained through the transformation of the above equations and the transfer of  $qx$  and  $qz$  to the left side.

$$qx = \rho g (2.61 a_H - 1/0.54 Z) \quad (3)$$

$$qz = \rho g (0.53 a_H - 1/2.18 z) \quad (4)$$

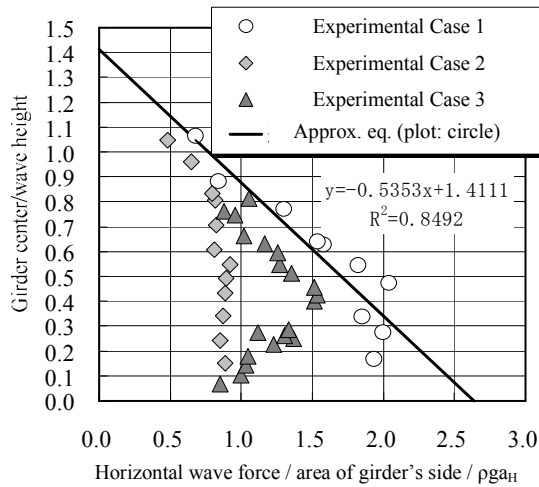


FIG. 15 RELATIONSHIP BETWEEN WAVE PRESSURE AND WATER PRESSURE OBTAINED FROM HORIZONTAL WAVE FORCE

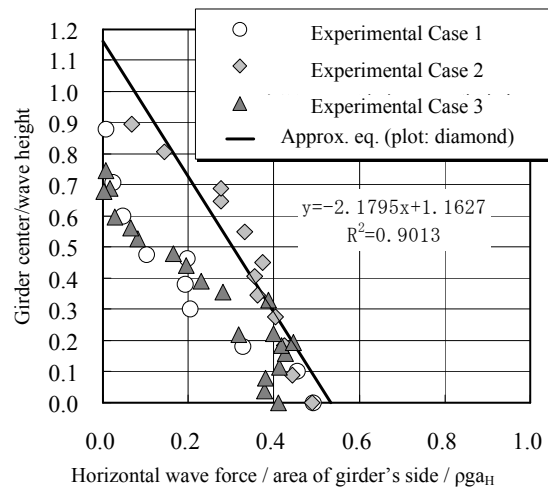


FIG. 16 RELATIONSHIP BETWEEN WAVE PRESSURE AND WATER PRESSURE OBTAINED FROM UPLIFT FORCE

### **Proposal of External Force Equation**

Equation (3) shows the wave pressure distribution of horizontal wave force and Equation (4) shows the vertical wave pressure distribution converted into the uplift force. The variables are the wave height and the girder position. If both of those values are known, the wave pressure can be calculated.

Figure 17 shows a schematic of wave pressure distribution and the external force calculation of Equations (3) and (4). As shown in the figure, the horizontal wave pressure distribution given by Equation (3) takes a triangle distribution form. The vertex is at a position 1.41 times the wave height  $a_H$  and the base on the static water level is 2.61 times the static water pressure against the wave height  $a_H$ . In this figure,  $Z1$  is the height up to the lower plane of the girder, which is called the girder height in this experiment.  $Z2$  is the height up to the bridge deck. If an integral equation having these variables is solved, the horizontal wave force is calculated. This triangular wave pressure distribution is smaller than the distribution which is obtained by the existing Goda's equation for wave force estimation.

Next, to obtain the uplift force, we assumed the condition in which the vertical wave pressure  $qz$  acts on the girder's lower plane uniformly. The distribution of the vertical wave pressure  $qz$  is obtained from a triangular distribution in which the vertex is at a position 1.16 times the wave height  $a_H$  and the base is 0.53 times the static water pressure against the wave height  $a_H$ . The uplift force is obtained by multiplying this vertical wave pressure  $qz$  by the width and length of the girder.

Based on the above, we propose the following equations as the equations for estimating the external forces of tsunami. Equation (5) is an equation for estimating the horizontal wave force  $Q_x$ . Equation (6) is an equation for estimating the uplift wave force  $Q_z$ .

$$Q_z = \rho g B W (0.53 a_H - 1/2.18 z) \quad (5)$$

$$Q_x = \rho g B \int_{z_1}^{z_2} (2.61 a_H - 1/0.54 Z) dZ \quad (6)$$

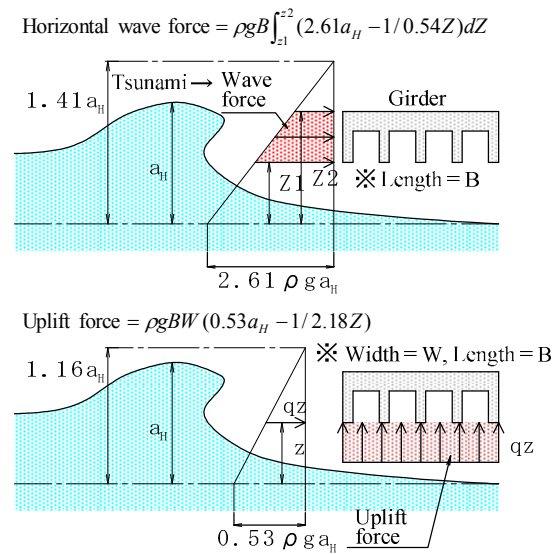


FIG. 17 SCHEMATIC OF TSUNAMI EXTERNAL FORCES  
(UPPER: HORIZONTAL WAVE FORCE, LOWER; UPLIFT FORCE)

## Conclusions

To identify the features of tsunami forces acting on bridges, we conducted an experiment using a 1/50 scale model resembling a damaged bridge in the 2004 Sumatra tsunami disaster. Based on the obtained results, we derived equations for estimating the horizontal wave force and the uplift wave force that act on the girder. From this study, the following conclusions were drawn.

1) According to the experiment on the wave actions on the girder, the horizontal wave force was large and the uplift force was small when the acting waves were broken. When the acting waves were not broken, the opposite trend was observed. When the acting waves consisted of both broken and unbroken waves, we could evaluate acting forces by dividing into broken and unbroken wave cases, although the effect varied by the position on the girder.

2) We proposed an estimation equation for each of the horizontal wave force and the uplift force. To derive those equations, we evaluated all experimental results using dimensionless values firstly and then derived a wave pressure distribution equation for each of the horizontal wave force and the uplift force from a wave pressure distribution line (linear approximate line) that covers the results of all experimental cases.

### **References**

1. Kosa, K., Nii, S., Shoji, M., and Kimura, K.: Experimental Study on Tsunami Waves Acting on Bridges, *Journal of Structural Engineering*, Vol. 55A, pp. 471-482, 2009 (in Japanese)
2. Unjoh, S.: Bridge Damage Caused by Tsunami, *Bulletin of Japan Association for Earthquake Engineering*, No. 6, pp. 26-28, 2007 (in Japanese)